PCCP



PAPER View Article Online
View Journal | View Issue



Cite this: Phys. Chem. Chem. Phys., 2014, 16, 20089

The influence of hydrogen bonding on the nonlinear optical properties of a semiorganic material $NH_4B[D-(+)-C_4H_4O_5]_2\cdot H_2O$: a theoretical perspective†

Chen Lei, ^{ab} Zhihua Yang, ^{*a} Bingbing Zhang, ^{ab} Ming-Hsein Lee, ^{ac} Qun Jing, ^{ab} Zhaohui Chen, ^a Xu-Chu Huang, ^{ab} Ying Wang, ^{ab} Shilie Pan*^a and Muhammad Ramzan Saeed Ashraf Janjua^{ad}

In this work, a potential semiorganic nonlinear optical candidate $NH_4B[D-(+)-(C_4H_4O_5)]_2\cdot H_2O$ (NBC) has been studied using Density Functional Theory. The origin of the second harmonic generation (SHG) effect of NBC crystals for the $NH_4B[D-(+)-(C_4H_4O_5)]_2\cdot H_2O$ molecular complex is explained by employing a combination of the density of states, SHG density and molecular orbital analysis. It reveals a way in which the organic and ammonium groups affect the SHG processes in a significantly different manner in the crystals and the molecular complex. In particular, the role of hydrogen bonding interaction in influencing the electronic structure and nonlinear optical properties is explicitly identified and explained.

Received 9th June 2014, Accepted 29th July 2014

DOI: 10.1039/c4cp02539c

www.rsc.org/pccp

1. Introduction

Nonlinear optical (NLO) materials are extensively studied because of their key role in laser technology and optical communication. Many inorganic NLO materials have commercial applications such as KDP (KH₂PO₄), KTP (KTiPO₅), LN (LiNbO₃), BBO (β-BaB₂O₄), LBO (LiB₃O₅), KBBF (KBe₂BO₃F₂), 6,7 AgGaS₂, ⁸AgGaSe₂, ⁹ ZnGeP₂¹⁰ and LiBC₂ (B = Al, Ga, In; C = S, Se, Te);^{11,12} in addition, some rising stars in inorganic NLO materials field, such as KBOC $(K_3B_6O_{10}Cl)$, ¹³ BBOF $(Ba_4B_{11}O_{20}F)$, ¹⁴ CsBSiO $(Cs_2B_4SiO_9)$, 15 CsZnBO $(Cs_3Zn_6B_9O_{21})$, 16 KAB $(K_2Al_2B_2O_7)^{17}$ and BaMgBO₃F, ¹⁸ are potential applicants. In addition, organic NLO materials attract attention due to their tailorability and remarkable SHG efficiency, which are 1-2 orders of magnitude larger than that of inorganic materials. The representative crystals DAST tosylate)19,20 (4-*N*,*N*-dimethylamino-4'-*N*'-methyl-stilbazolium and MMONS (3-methyl-4-methoxy-4'-nitrostilbene)21,22 exhibit excellent SHG efficiency, which implies that they have significant

To design superior NLO compounds, a series of organic-inorganic hybrid compounds with $(C_4H_4O_5)$ -type fundamental building units and alkali-metal or ammonium groups, such as NaB(DL-C₄H₄O₅)₂,³¹ NaB(L-C₄H₄O₅)₂,³² RbB(DL-C₄H₄O₅)₂·H₂O (RBC),³³ NH₄B[D-(+)-C₄H₄O₅]₂·H₂O (NBC)³⁴ and CsB(DL-C₄H₄O₅)₂·H₂O, H₂O,³¹ were synthesized *via* a slow evaporation method. The compounds, except for CsB(DL-C₄H₄O₅)₂·H₂O, possess noncentrosymmetric space group with the SHG intensities about 1–2 times that of KDP. Investigating these organic–inorganic compounds will provide references for designing new materials. Therefore, understanding the relationship between microscopic structure and macroscopic optical properties is quite interesting ^{35–39} because of two main reasons: first, introducing high hyperpolarizability semiorganic molecules appears to be an effective method for

potential applications in biological imaging,²³ all-optical switching²⁴ and logic devices,²⁵ *etc.* However, there exists a wide gap between experimental research and commercial use due to their limitations in physico-chemical stability.²⁶ Because of the natural advantage over organic and inorganic NLO materials, semi-organic NLO crystals are expected to become superior candidates. Thus, many types of semiorganic materials were synthesized and applied.^{26,27} For example, LFM (HCOOLi·H₂O)²⁸ shows 20 times larger SHG response than that of KDP, and it has been used in multiple frequency components in the 1980s. LAP (L-arginine phosphate monohydrate) possesses a larger NLO response and higher laser damage threshold than the inorganic crystal KDP, and therefore it has been applied in ultrafast pulse and laser doubling techniques.^{29,30} Here, we are interested in boron-based organic–inorganic hybrid compounds.

^a Key Laboratory of Functional Materials and Devices for Special Environments of CAS, Xinjiang Technical Institute of Physics & Chemistry of CAS, Xinjiang Key Laboratory of Electronic Information Materials and Devices, 40–1 South Beijing Road, Urumqi 830011, China. E-mail: zhyang@ms.xjb.ac.cn, slpan@ms.xjb.ac.cn; Fax: +86-991-3835096; Tel: +86-991-3810816

^b University of Chinese Academy of Sciences, Beijing 100049, China

^c Department of Physics, Tamkang University, Taipei 25137, Taiwan

^d Department of Chemistry, University of Sargodha, Sargodha-40100, Pakistan

[†] Electronic supplementary information (ESI) available: The band structure of the NBC crystal, the structure of the NBC molecular complex and the molecular complex with hydrogen bonds and the table of contributions of SHG coefficients of different transitions for NBC crystal. See DOI: 10.1039/c4cp02539c

Paper

obtaining new semiorganic NLO compounds, although this strategy is insufficient to obtain noncentrosymmetric structures; second, the process of crystal engineering based on molecular properties is unexplained; thus, a comprehensive study of the microstructure–structure–property relationship is still required to explore optimized materials.

This work emphasizes exploring the origin of the SHG effect. Here, the NBC crystal linked through hydrogen bonding in molecules, as a new material having the weakest interaction between molecules in the series of materials previously mentioned, was studied as a demonstration. Because of the weak interaction, the molecular design could be expected to be the crystal design. In addition, the research of the SHG effect source for NBC is beneficial for providing some inspiration to design new NLO crystals. In this work, we first introduce the crystal structure and properties followed by a microscopic analysis for understanding the origin of the SHG effect both at the crystal and molecular level, which is presented in terms of the density of states and SHG density⁴⁰ by a plane-wave pseudopotential method of density functional theory (DFT). Finally, the difference of the SHG origin between the crystal and molecular complex is discussed, and the influence of hydrogen bonding interaction on the electronic structure and optical properties are further elaborated.

2. Calculation methods

To explore the origin of the SHG effect in NBC crystals, the electronic structure and the optical property calculations were performed using the DFT method implemented in the CASTEP package. The local-density approximation (LDA) was adopted using Ceperley and Alder–Perdew and Zunger (CA–PZ) functional for studying the exchange–correlated interactions. Norm-conserving pseudopotentials were set, and valence electrons were provided by the package used. The number of plane waves included in the study was determined by a cutoff energy of 830 eV, and the numerical integration of the Brillouin zone was performed using a 3 × 6 × 2 Monkhorst–Pack k-point sampling. The real part ε_1 and the imaginary parts ε_2 of the dielectric function were calculated within the CASTEP package. The expression of the imaginary parts ε_2 is as follows:

$$arepsilon_{2}(\hbar\omega)=rac{2e^{2}\pi}{Varepsilon_{0}}\sum_{k,
u,c}\left|\left\langle \psi_{k}^{c}\left|\widehat{u}\cdot\overrightarrow{r}\right|\psi_{k}^{
u}
ight
angle \right|^{2}\deltaig(E_{k}^{c}-E_{k}^{
u}-\hbar\omegaig)$$

where ν and c are valance band (VB) and conduction band (CB) indices, respectively. \widehat{u} represents the polarization of the electric field, ω is the frequency of incident light, V is the volume of cell, and \overrightarrow{r} is the position operator, which is expressed as momentum matrix to satisfy the crystalline boundary condition used in the CASTEP package. The real and imaginary parts are linked by a Kramers–Kronig transformation, ⁴⁹ and the real part can be obtained from this transformation. The linear optical properties can be defined based on the dielectric functions.

Moreover, SHG coefficients were calculated at a zero-frequency limit by the length-gauge formalism derived by

Aversa and Sipe.⁵⁰ The static second-order nonlinear susceptibilities $\chi_{\alpha\beta\gamma}^{(2)}$ can be reduced as follows:

$$\chi_{\alpha\beta\gamma}^{(2)} = \chi_{\alpha\beta\gamma}^{(2)}(VE) + \chi_{\alpha\beta\gamma}^{(2)}(VH) + \chi_{\alpha\beta\gamma}^{(2)}(two bands), \qquad (2)$$

where α , β , and γ are Cartesian components, $\chi^{(2)}_{\alpha\beta\gamma}(\text{VE})$, $\chi^{(2)}_{\alpha\beta\gamma}(\text{VH})$ and $\chi^{(2)}_{\alpha\beta\gamma}(\text{two-bands})$ denote the contributions from virtual-electron (VE), virtual-hole (VH) and two-band processes to $\chi^{(2)}_{\alpha\beta\gamma}$, respectively.

Results and discussion

3.1. Crystal structure

NBC holds the space group $Pna2_1$ with lattice parameters a = 11.4846 Å, b = 5.3543 Å, and c = 21.0791 Å. The $[B(D-(+)-C_4H_4O_5)_2]^-$ groups (Fig. 1(a)) can be treated as the fundamental building units (FBUs), which can be described as two malic acid molecules linked by a BO₄ tetrahedron. Then, NH₄⁺ groups and H₂O molecules connect the $[B(D-(+)-C_4H_4O_5)_2]^-$ groups with N-H···O and O-H···O hydrogen bonds, respectively, (Fig. 1(b)).

Each B atom is bonded to four O atoms to form BO_4 units, and each BO_4 tetrahedron is bridged by two malate groups in the *cis*-position. The B–O distance ranges from 1.416 to 1.519 Å with O–B–O angle ranging from 103.9° to 114.5°. The length of N–H···O hydrogen bonds ranges from 1.889 to 2.556 Å and O–H···O hydrogen bonds length ranges from 1.805 to 1.978 Å. The minimum of N–H···O hydrogen bonding angle is 142.703°, and the maximum is 169.837°. For O–H···O, the bond angle shows two values, 169.588° and 176.286°.

In the structural aspect of these series of organic–inorganic hybrid compounds, the alkali metal atom radius affecting the alignment of FBUs may be an important factor for crystal structure. By the comparison of these compounds it can be concluded that the basic anion $[B(\text{p-}(+)-\text{C}_4\text{H}_4\text{O}_5)_2]^-$ has similar structure and different arrangement mode due to the difference in cations. Interestingly, the RbB(pl-C₄H₄O₅)₂·H₂O compound

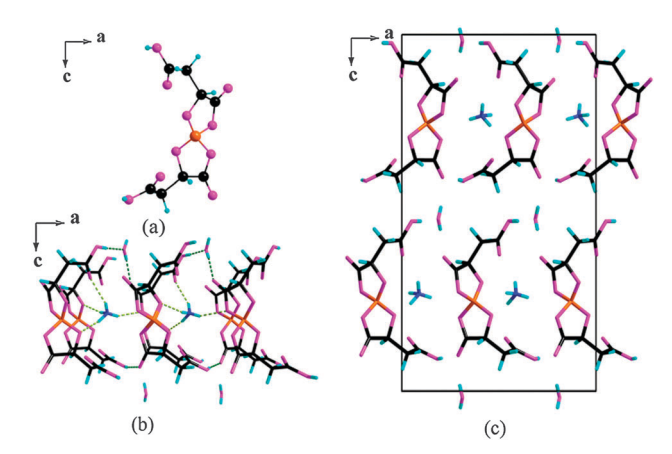


Fig. 1 Structure of NBC. Pink colour denotes the oxygen atom, black color represents the carbon atom, dark blue indicates nitrogen and light blue represents the hydrogen atom; (a) FBU: the $[B(D-(+)-C_4H_4O_5)_2]^-$ group. (b) Hydrogen bonding among FBUs: the green bond presents the O–H···O and the light green presents N–H···O. (c) Crystal structure viewed in the [010] face.

PCCP

is the isostructure of NBC but the compound CsB(DL-C₄H₄O₅)₂. H₂O is centrosymmetric, which demonstrates the influence of alkali-metal cations on structural modification.

3.2. Optical properties

The calculated band structure (Fig. S1, ESI†) shows an indirect band gap of 4.58 eV for NBC with the bottom of CBs located at Γ point and the top of VBs at U point. This calculated band gap is slightly less than the experimental value of 5.28 eV, which is reasonable because the band gap is generally underestimated in the band structure calculation with DFT in both LDA and GGA of Kohn Sham implementation. 51-54 The wide band gap indicates that NBC is a potential crystal in the UV region. Considering that optical properties are studied based on the electronic structure calculation, a corrected scissor defined as the difference between experimental and calculated results is required for the calculation of optical properties.

Here, the dielectric function is discussed to enrich the study of properties and further confirm the reliability of the calculation. There are three nonzero dielectric functions $(\varepsilon_x, \varepsilon_y, \varepsilon_z)$ in X, Y, Z directions for NBC because it crystallizes in mm2 point group, which belongs to low symmetry crystal systems. The real part of $\varepsilon(\omega)$ in the limit of infinite wavelength is equal to the square of refractive index n, and the imaginary part reflects the transition between the occupied and unoccupied bands. The frequencydependent dielectric functions along three principal dielectric axes of NBC in Fig. 2 clearly show anisotropic behavior along different

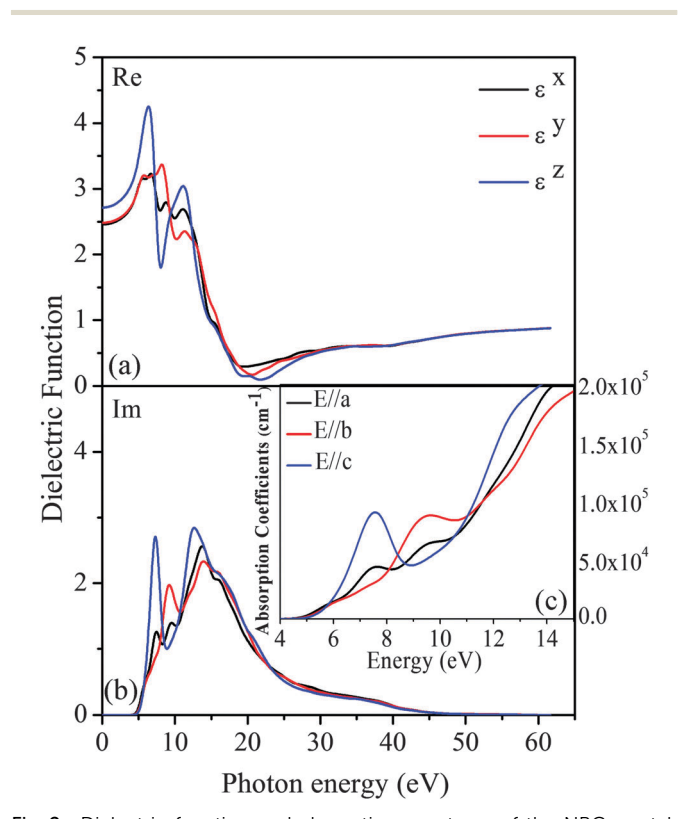


Fig. 2 Dielectric function and absorption spectrum of the NBC crystal. (a)The real parts of dielectric function, (b) the imaginary part of dielectric function and (c) the absorption spectrum.

dielectric axes. The calculated static dielectric constants $\operatorname{Re}[\varepsilon^{x}(\omega=0)], \operatorname{Re}[\varepsilon^{y}(0)], \text{ and } \operatorname{Re}[\varepsilon^{z}(0)] \text{ are } 2.481, 2.483 \text{ and } 2.714,$ respectively, which characterize the dielectric response in the static electric field. The tendency of the imaginary part of dielectric function indicates that electronic transitions arising from VBs to CBs are responsible for the intrinsic UV absorption α . As shown in Fig. 2(c), several peaks are apparently attributed to electronic transitions within the sub-bands. Moreover, the optical absorption coefficient spectrum shows the calculated absorption edge similar to the experimental edge of 235 nm, which indicates the reliability of DFT calculations.

NBC is a biaxial crystal and the corresponding relationship between the dielectric and the crystallographic axes are $X \to a$, $Y \rightarrow b$, $Z \rightarrow c$. The computed refractive indices n1, n2 and n3 are 1.515, 1.516 and 1.608 at 1064 nm, respectively. The birefringence of the NBC ranges approximately from 0.092 to 0.093 in the region from the UV-Vis to 1064 nm. This birefringence is comparable to those of the well-known crystals such as BBO, urea and LN with birefringence values of 0.1125, 0.1019 and 0.076 at 1064 nm, respectively.

The SHG response with experimental powder using the Kurtz-Perry method for NBC is 1.5 times that of KDP,34 and the corresponding effective second-order nonlinear coefficient is about 1.2 times that of KDP. The calculated coefficients at zero frequency limit are $|d_{15}| = 0.33$ KDP $(d_{36}$ for KDP = 0.39 pm V⁻¹), $|d_{24}| = 0.27$ KDP, and $|d_{33}| = 0.88$ KDP. To investigate the origin of the NLO effect, the microstructureelectronic structure-property relationship was studied. Hereafter, the coefficient d_{15} has been chosen as a representative because the d_{15} , d_{24} , and d_{33} have similar properties.

3.3. Origin of the SHG response

The study of electronic structure is very helpful to understand structural configurations and to explore the mechanism of the SHG response for the NBC. Partial density of states (PDOS) near the Fermi energy level was displayed because the optical properties of a crystal in the UV and visible spectra were mainly determined by the states close to the band gap. Furthermore, based on the metal properties of ammonium, NH₄⁺ is treated as an independent unit for further discussions. As shown in Fig. 6(a), the s and p orbitals of the NH₄⁺ group are located in the region ranging from -10 to -5 eV and the region above 6 eV. Both the top of the VB and the bottom of the CB are mainly occupied by O 2p orbitals, C 2p orbitals and slightly occupied by H 1s orbitals of hydrogen atoms, except for those of ammonium. It is clarified that the orbitals of oxygen and carbon atoms are the dominant factors in electronic transition, which is considered to be the intrinsic reason for the SHG response. It indicates that ammonium has no significant direct impact on the SHG effect.

To reveal the contribution of different atoms in the SHG process in real space, the SHG density of the NBC has been analyzed under band resolve framework.55 Importantly, the contributions of different transitions to the SHG effects are calculated (Table S1, ESI†). The contribution of the virtual electron (VE) processes to the SHG effects are 104.88%,

Paper

164.32%, and 56.29% for d_{15} , d_{24} , and d_{33} , respectively, whereas the virtual hole (VH) contributes -4.88%, -64.32% and 43.71% to d_{15} , d_{24} and d_{33} , respectively. It shows that the VE processes make dominant contributions toward the SHG effect.

Fig. 3 shows the density of the SHG effect in unoccupied and occupied states of VE processes, which exhibits the dominant contribution toward the SHG coefficient in real space. For unoccupied states, Group I of [-C(7)OOH] and Group IV of [-C(3)OO-] offer positive contributions to the SHG response, whereas Group II of [-C(4)OO-] and Group III of [-C(2)OOH] have negative contributions. In addition, the superposition of Groups I and II consisting of $[B(C_4H_4O_5)_2]^-$ connected by B(1) is the main contributor to the SHG effect. For occupied states, Group IV of the [-C(7)OOH] group and H_2O molecule have positive contributions. It is clear from the abovementioned discussion, the $[B(D-(+)-C_4H_4O_5)_2]^-$ group plays a dominant role in the SHG effect whereas NH_4^+ has no direct contribution to the SHG effect.

As we have previously mentioned in the SHG densities, the SHG effect for crystal is a localized effect and is consequently attributed to the contribution from some fundamental units; thus, the $NH_4B[D-(+)-C_4H_4O_5]_2\cdot H_2O$ molecular complex, which consists of a $B[D-(+)-C_4H_4O_5]_2$ group and its nearest neighbor the H_2O molecule and NH_4 forming the lowest energy complex as the repeating unit of the NBC crystal (as shown in Fig. S2, ESI†), is studied to explore the origin of the SHG effect. In addition, the NLO effect at the molecular level is usually believed to be based on the charge transfer mechanism, for and molecular orbitals are regarded as powerful tools to indicate possible charge transfer. Thus, the molecular orbitals of $NH_4B[D-(+)-C_4H_4O_5]_2\cdot H_2O$ molecular complex from the DFT method implemented by Gaussian09 package⁵⁷ at B3LYP/6-31+G(d,p) level are used to demonstrate charge transfer in

(a)
-1.197e-1
-7.498e-2
-3.026e-2
-1.447e-2
--5.920e-2

(b)
-1.358e-1
-1.019e-1
-6.792e-2
-3.396e-2

Fig. 3 SHG densities of d_{15} tensor component. (a) VE unoccupied, and (b) VE occupied. The value near zero is not shown in the figure to reveal the main influence group.

closely related atoms. Moreover, the SHG density of the molecular complex was also calculated using the same condition as in the case of crystal to show the source of the SHG.

According to the frontier molecular orbitals (FMO) theory, HOMO (highest occupied molecular orbital) and LUMO (lowest unoccupied molecular orbital) are very important to optical properties. The frontier molecular orbitals of the $NH_4B[D-(+)-C_4H_4O_5]_2$. H_2O molecular complex was investigated to demonstrate the influence of orbitals on the SHG effect. As shown in Fig. 4, it is

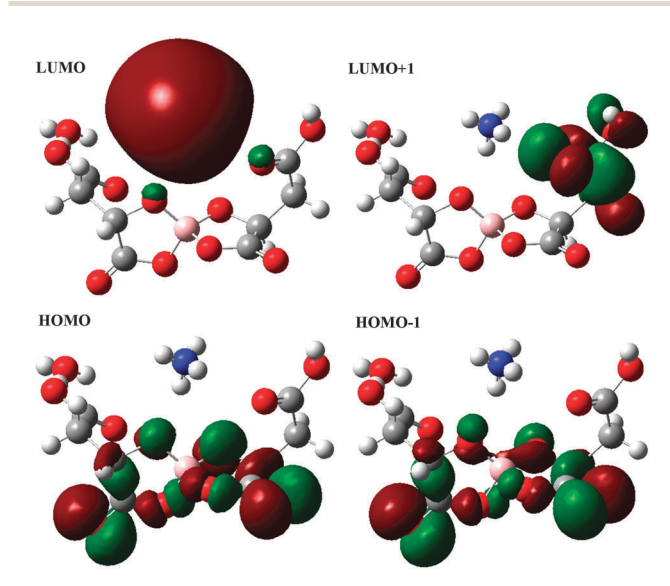


Fig. 4 Frontier molecular orbitals (FMOs) of the NH $_4$ B[D-(+)-C $_4$ H $_4$ O $_5$] $_2$ ·H $_2$ O molecular complex.

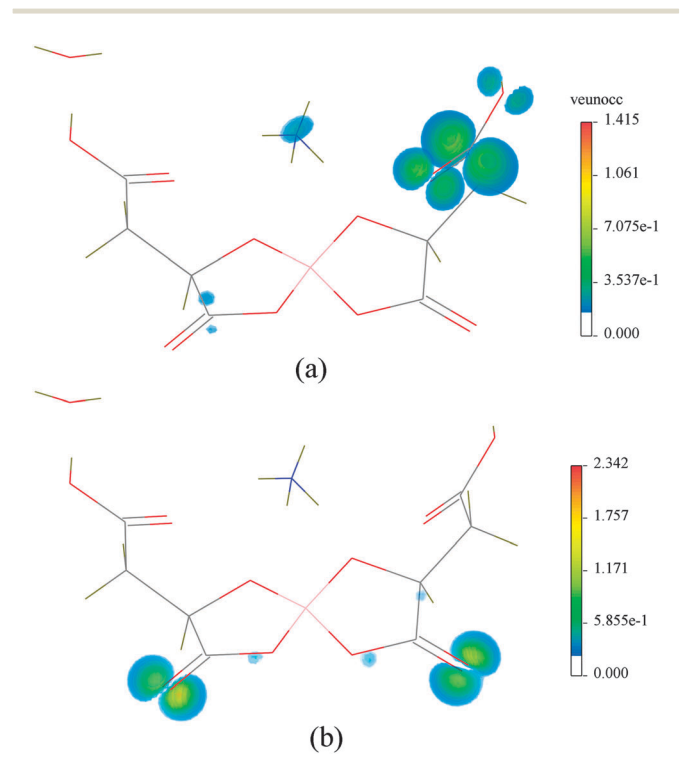


Fig. 5 SHG density of the NH $_4$ B[D-(+)-C $_4$ H $_4$ O $_5$] $_2$ ·H $_2$ O molecular complex in NBC: (a) the VE unoccupied states, (b) the VE occupied states.

PCCP

illustrated that both HOMO and HOMO - 1 are occupied by two adjacent five-membered rings consisting of one BO4 group and two carbon chains; LUMO is localized on the NH4+ group and LUMO + 1 is localized on the nearby organic part (-CH₂COOH) that includes a carboxyl and a CH2 group. As a result, a conclusion has been drawn that the charge transfer from the $[B(C_4H_4O_5)_2]^-$ to the ammonium is crucial for the SHG effect, which demonstrates that the contribution from both the organic and the ammonium part to molecular properties cannot be neglected. SHG densities of the NH₄B[D-(+)-C₄H₄O₅]₂·H₂O molecular complex has also been calculated (Fig. 5); the molecular complex was placed in a 25 \times $25 \times 30 \text{ Å}$ vacuum box to avoid interaction between two neighboring images. It is shown that the active parts in the occupied states and unoccupied states in the SHG densities is similar to that of its HOMO, HOMO - 1 and LUMO, LUMO + 1 molecular orbitals, which again confirms that both the $[B(C_4H_4O_5)_2]^-$ and NH_4^+ play significant roles toward molecular optical properties. Clearly, this result is different from the conclusion of the crystalline calculation that shows ammonium has no contribution to the NLO effect. From the SHG density, the contribution of ammonium appears in unoccupied states for microscopic units but not for crystal. Moreover, [-C(3)OO-] and [-C(4)OO-] groups have an apparent

contribution to crystal unoccupied states but only a slight contribution in the molecular complex case.

On comparing the crystalline with the molecular complex, we can find that the hydrogen bonding distribution is clearly different. The crystal is formed by linking molecules with hydrogen bonding. Therefore, hydrogen bonding interaction may be a key factor that leads to the difference between the molecular complex and the crystal. To clarify the influence of hydrogen bonding, the molecular complex and the crystal was compared to show the influence of hydrogen bonding. [-C(3)OO-] and [-C(4)OO-] groups were treated as a unit because of their similar tendency in the SHG densities. As shown in Fig. 6, ammonium has apparent differences in CBs of the crystal and NH₄B[D-(+)-C₄H₄O₅]₂·H₂O molecular complex. In crystal, ammonium has almost no contribution to the density of states (DOS) at the bottom of CBs. Whereas for the molecular complex, a remarkable peak is derived from s and p orbitals of ammonium at the bottom of CBs. During the formation of the crystal, the hydrogen bonding interaction between coordinated oxygen atoms and ammonium weakens the contribution of ammonium orbitals near the bottom of the CBs. On the contrary, the formation of hydrogen bonds between H2O molecules and

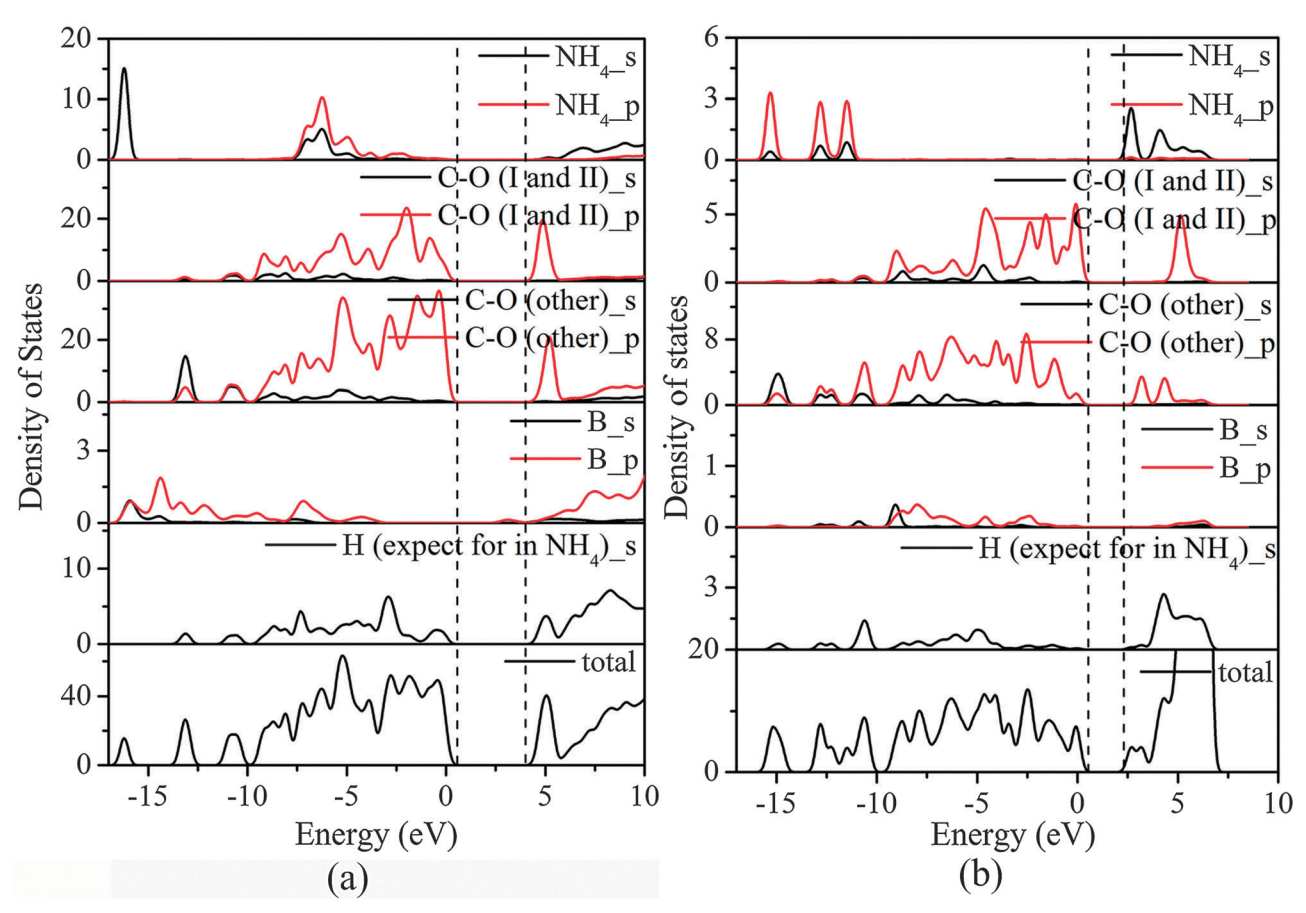


Fig. 6 PDOS of the NBC crystal and the NH $_4$ B[D-(+)-C $_4$ H $_4$ O $_5$] $_2$ ·H $_2$ O molecular complex. (a) PDOS of crystal and (b) PDOS of the NH $_4$ B[D-(+)-C $_4$ H $_4$ O $_5$] $_2$ ·H $_2$ O molecular complex; the C-O (I and II) represents carbon and oxygen atoms in Group I and Group II defined in Fig. 3, C-O (other) represents carbon and oxygen atoms except for those in group I and II, and the H atoms in the fifth panel represent hydrogen atoms except for the hydrogen atoms in ammonium. The left dotted line is the boundary of the VB and the right one is the boundary of the CB. Notice the difference between (a) and (b) in the top three panels.

terminal oxygen atoms in Group I and II makes p orbitals of both O and C atoms in CB to appear in the same energy region. The N-H···O and O-H···O hydrogen bonding in the NBC crystal changes the electronic distribution and may be an important factor in determining the origin of the SHG for the NBC crystal.

To further prove the importance of hydrogen bonding in the NBC crystal, molecular complexes with and without surrounding hydrogen bonds were investigated. The hydrogen bonding interaction was considered by linking ammonium and water molecules to the organic group, which is treated as the group with hydrogen bonds (Fig. S3, ESI†) and the group of B[D-(+)-C₄H₄O₅]₂ (Fig. 1(a)) is treated as the group without hydrogen bonds. The molecular complexes were placed in 25 \times 25 \times 30 Å

vacuum boxes to avoid interaction between the two neighboring images. The calculated SHG densities of the group with and without hydrogen bonds are compared with the SHG densities of the NBC crystal.

According to the SHG densities of the NBC crystal (Fig. 7(e) and (f)), Group I and Group IV dominate the contribution of unoccupied states, whereas the O(8) and O(9) atoms are crucial for the contribution of occupied states. Fig. 7(a) and (c) show that the hydrogen bonding interaction makes Group I and Group IV of the molecular complex recover their predominant status and play the most important role similar to crystal. Moreover, Fig. 7(b) and (d) indicate that the hydrogen bonding interaction makes both O(8) and O(9) to have a significant contribution and weaken the contribution of O(1), O(4), O(6)

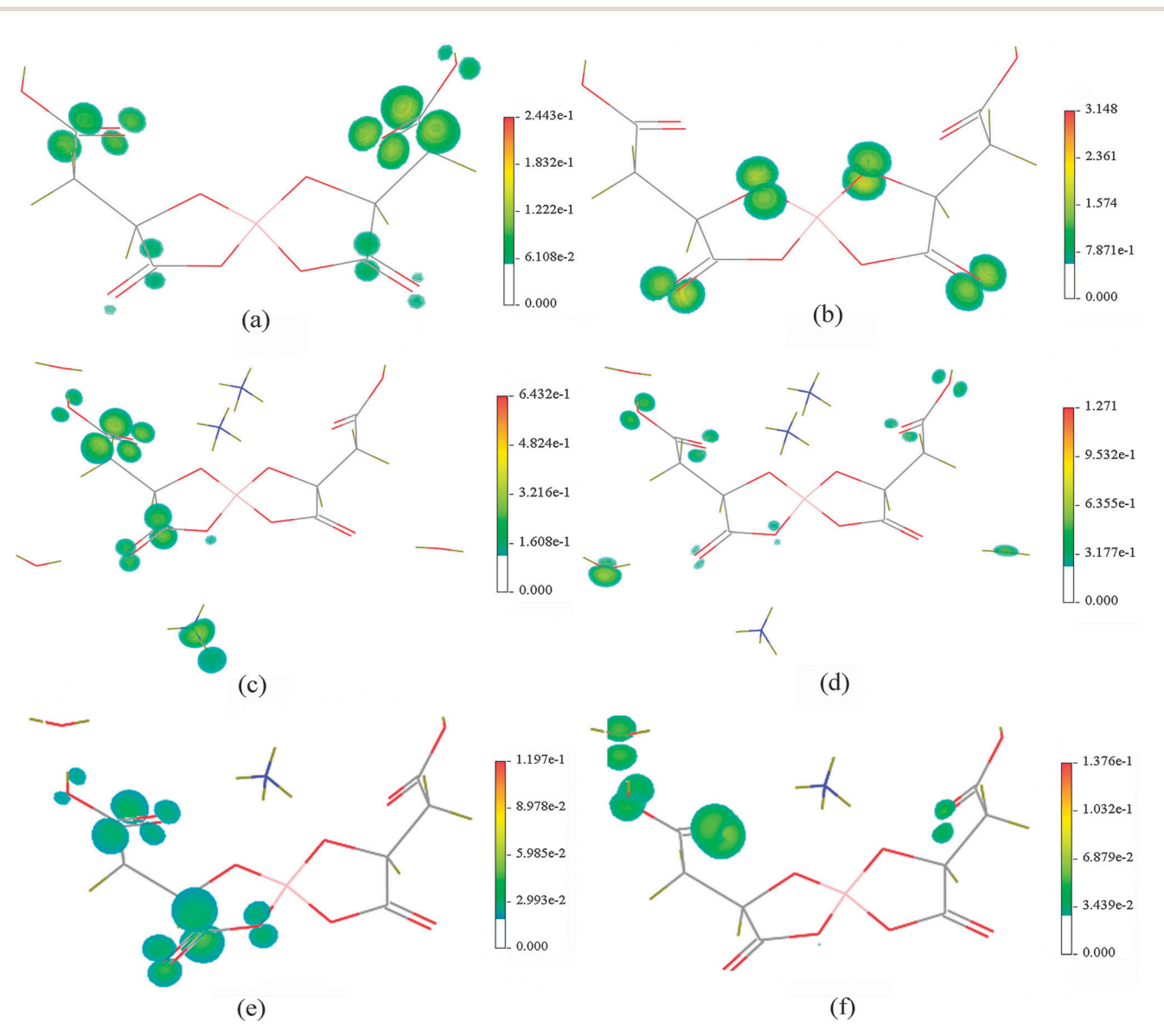


Fig. 7 SHG densities of the molecular complex with and without hydrogen bonds and that of the NBC crystal. (a) and (b) present the VE unoccupied states and VE occupied states for the d_{15} component of the SHG densities of the molecular complex without the hydrogen bond, respectively; (c) and (d) present the VE unoccupied states and VE occupied states for the d_{15} component of the molecular complex with hydrogen bonds, respectively; (e) and (f) present the VE unoccupied states and VE occupied states for the d_{15} component of the NBC crystal, respectively.

PCCP Paper

and O(7) in occupied states, which is closer to the tendency of its crystalline counterpart. Based on the abovementioned analysis, the SHG densities of the complex with hydrogen bonds show a tendency much more similar to the crystal than that of the complex without hydrogen bonds. Therefore, hydrogen bonding interaction is the key factor that leads to a difference in the source of the SHG effect between the molecular complex and the crystal.

4. Conclusions

In conclusion, the properties of an organic–inorganic hybrid nonlinear optical material NBC are calculated by employing the plane-wave pseudopotential DFT method in the CASTEP package. The electronic structure and FMOs have been investigated to explore the origin of NLO properties. In the exploration of the origin of the SHG in the NBC, three conclusions are drawn: (1) for the NBC crystal, the [B(D-(+)-C₄H₄O₅)₂]⁻ group is dominant, and ammonium has no significant direct contribution to NLO properties; (2) the repeating unit NH₄B[D-(+)-C₄H₄O₅]₂·H₂O molecular complex was studied, and the result has shown that such isolated organic fragments have a different NLO-active substructure compared to that in the crystal; (3) hydrogen bonding has significant indirect influence on the SHG effect for the NBC crystal by changing the electronic distribution of the atoms involved in hydrogen bonding.

Acknowledgements

This work is supported by the "Western Light Joint Scholar Foundation" Program of Chinese Academy of Sciences (Grant No. LHXZ201101), the National Key Basic Research Program of China (Grant No. 2014CB648400), the "National Natural Science Foundation of China" (Grant No. 11104344, 51202210) and the High-level Professional and Technical Personnel of Autonomous region. MHL thanks NCHC for database support and Keywin Electronic Inc. for equipment donation.

Notes and references

- 1 J. J. De Yoreo, A. K. Burnham and P. K. Whitman, *Int. Mater. Rev.*, 2002, 47, 113–152.
- 2 A. H. Reshak, I. V. Kityk and S. Auluck, *J. Phys. Chem. B*, 2010, **114**, 16705–16712.
- 3 G. D. Boyd, K. Nassau, R. C. Miller, W. L. Bond and A. Savage, *Appl. Phys. Lett.*, 1964, 5, 234–236.
- 4 C. Chen, B. Wu, A. Jiang and G. You, *Sci. Sin., Ser. B* (*Engl. Ed.*), 1985, **28**, 235–241.
- 5 C. Chen, Y. Wu, A. Jiang, B. Wu, G. You, R. Li and S. Lin, J. Opt. Soc. Am. B, 1989, 6, 616–621.
- 6 C. Chen, G. Wang, X. Wang and Z. Xu, *Appl. Phys. B: Lasers Opt.*, 2009, **97**, 9–25.
- 7 B. Wu, D. Tang, N. Ye and C. Chen, *Opt. Mater.*, 1996, 5, 105–109.

- 8 A. Harasaki and K. Kato, *Jpn. J. Appl. Phys.*, 1997, 36, 700–703.
- 9 G. C. Catella, L. R. Shiozawa, J. R. Hietanen, R. C. Eckardt, R. K. Route, R. S. Feigelson, D. G. Cooper and C. L. Marquardt, *Appl. Opt.*, 1993, 32, 3948–3951.
- 10 G. D. Boyd, E. Buehler and F. G. Storz, Appl. Phys. Lett., 1971, 18, 301–304.
- 11 L. Isaenko, I. Vasilyeva, A. Merkulov, A. Yelisseyev and S. Lobanov, *J. Cryst. Growth*, 2005, 275, 217–223.
- 12 L. Isaenko, A. Yelisseyev, S. Lobanov, A. Titov, V. Petrov, J. J. Zondy, P. Krinitsin, A. Merkulov, V. Vedenyapin and J. Smirnova, *Cryst. Res. Technol.*, 2003, 38, 379–387.
- 13 H. Wu, S. Pan, K. R. Poeppelmeier, H. Li, D. Jia, Z. Chen, X. Fan, Y. Yang, J. M. Rondinelli and H. Luo, *J. Am. Chem. Soc.*, 2011, 133, 7786–7790.
- 14 H. Wu, H. Yu, Z. Yang, X. Hou, X. Su, S. Pan, K. R. Poeppelmeier and J. M. Rondinelli, J. Am. Chem. Soc., 2013, 135, 4215–4218.
- 15 H. Wu, H. Yu, S. Pan, Z. Huang, Z. Yang, X. Su and K. R. Poeppelmeier, *Angew. Chem., Int. Ed.*, 2013, 52, 3406–3410.
- 16 H. Yu, H. Wu, S. Pan, Z. Yang, X. Hou, X. Su, Q. Jing, K. R. Poeppelmeier and J. M. Rondinelli, *J. Am. Chem. Soc.*, 2014, 136, 1264–1267.
- 17 Z. Hu, T. Higashiyama, M. Yoshimura, Y. K. Yap, Y. Mori and T. Sasaki, *Jpn. J. Appl. Phys.*, *Part* 2, 1998, 37, L1093–L1094.
- 18 J. Zhao, M. Xia and R. K. Li, J. Cryst. Growth, 2011, 318, 971-973.
- 19 S. R. Marder, J. W. Perry and C. P. Yakymyshyn, *Chem. Mater.*, 1994, **6**, 1137–1147.
- 20 M. Jazbinsek, L. Mutter and P. Gunter, *IEEE J. Sel. Top. Quantum Electron.*, 2008, **14**, 1298–1311.
- 21 T. Wilson, G. Brigitte, C. C. Joseph and H. S. Sylvia, *Chem. Phys. Lett.*, 1989, **154**, 3–96.
- 22 H.-k. Hong, J. W. Park, K.-S. Lee and C. Sup Yoon, *J. Cryst. Growth*, 2005, 277, 509–517.
- 23 S. Fan, F. Qi, T. Notake, K. Nawata, T. Matsukawa, Y. Takida, H. Minamide, Proc. SPIE 8964, Nonlinear Frequency Generation and Conversion: Materials, Devices, and Applications XIII, 896401, February 5, 2014.
- 24 R. L. Gieseking, S. Mukhopadhyay, C. Risko, S. R. Marder and J.-L. Brédas, *Adv. Mater.*, 2014, 26, 68–84.
- 25 Z.-Y. Li and Z.-M. Meng, J. Mater. Chem. C, 2014, 2, 783–800.
- 26 M. Jiang and Q. Fang, Adv. Mater., 1999, 11, 1147-1151.
- 27 C. Chen, X. Sun, F. Wang, F. Zhang, H. Wang, Z. Shi, Z. Cui and D. Zhang, *IEEE J. Quantum Electron.*, 2012, 48, 61–66.
- 28 S. Singh, W. A. Bonner, J. R. Potopowi and L. G. Vanuiter, *Appl. Phys. Lett*, 1970, 17, 292–294.
- 29 A. Yokotani, T. Sasaki, K. Yoshida and S. Nakai, *Appl. Phys. Lett.*, 1989, 55, 2692–2693.
- 30 A. Yokotani, T. Sasaki, K. Fujioka, S. Nakai and C. Yamanaka, J. Cryst. Growth, 1990, 99, 815–819.
- 31 H. Huang, W. Yao, Z. Lin, Y. He, N. Tian, C. Chen and Y. Zhang, *J. Alloys Compd.*, 2014, **582**, 374–379.
- 32 H. Huang, W. Yao, Y. He, N. Tian, C. Chen and Y. Zhang, *Mater. Res. Bull.*, 2013, **48**, 3077–3081.

- 33 Z. Chen, S. Pan, H. Wu, Y. Yang and X. Fan, *Mater. Chem. Phys.*, 2011, **129**, 649–653.
- 34 Z. Chen, S. Pan, Q. Jing, Y. Yang, X. Dong, Q. Bian, J. Han, L. Dong and Z. Yang, Z. Anorg. Allg. Chem., 2014, 640, 140–146.
- 35 H. L. Xu, Z. R. Li, D. Wu, B. Q. Wang, Y. Li, F. L. Gu and Y. Aoki, *J. Am. Chem. Soc.*, 2007, **129**, 2967–2970.
- 36 S. Muhammad, H.-L. Xu, R.-L. Zhong, Z.-M. Su, A. G. Al-Sehemi and A. Irfan, J. Mater. Chem. C, 2013, 1, 5439–5449.
- 37 Y. Y. Hu, S. L. Sun, W. T. Tian, W. Q. Tian, H. L. Xu and Z. M. Su, *ChemPhysChem*, 2014, 15, 929–934.
- 38 R. L. Zhong, J. Zhang, S. Muhammad, Y. Y. Hu, H. L. Xu and Z. M. Su, *Chem. Eur. J.*, 2011, 17, 11773–11779.
- 39 D. L. Wang, H. L. Xu, Z. M. Su and G. Xin, *Phys. Chem. Chem. Phys.*, 2012, 14, 15099–15105.
- 40 C.-H. Lo, Master Degree Thesis, Tamkang University, 2005.
- 41 S. J. Clark, M. D. Segall, C. J. Pickard, P. J. Hasnip, M. J. Probert, K. Refson and M. C. Payne, *Z. Kristallogr.*, 2005, **220**, 567–570.
- 42 D. M. Ceperley and B. J. Alder, *Phys. Rev. Lett.*, 1980, 45, 566–569.
- 43 S. N. Rashkeev, W. R. L. Lambrecht and B. Segall, *Phys. Rev. B: Condens. Matter Mater. Phys.*, 1998, 57, 3905–3919.
- 44 M.-H. Lee, PhD thesis, The University of Cambridge, 1996.
- 45 J. Lin, A. Qteish, M. C. Payne and V. Heine, *Phys. Rev. B: Condens. Matter Mater. Phys.*, 1993, 47, 4174–4180.

- 46 A. M. Rappe, K. M. Rabe, E. Kaxiras and J. D. Joannopoulos, Phys. Rev. B: Condens. Matter Mater. Phys., 1990, 41, 1227–1230.
- 47 M.-H. Lee, J.-S. Lina, M. C. Paynea, V. Heinea, V. Milmana and S. Crampina, *Psi-k Newsletters*, 2005, **67**, 145–159.
- 48 H. J. Monkhorst and J. D. Pack, *Phys. Rev. B: Condens. Matter Mater. Phys.*, 1976, 13, 5188–5192.
- 49 E. D. Palik, *Handbook of Optical Constants of Solids*, Academic Press, Orlando New York, 1985.
- 50 C. Aversa and J. E. Sipe, *Phys. Rev. B: Condens. Matter Mater. Phys.*, 1995, 52, 14636–14645.
- 51 L. J. Sham and M. Schluter, *Phys. Rev. Lett.*, 1983, 51, 1888–1891.
- 52 P. Mori-Sanchez, A. J. Cohen and W. T. Yang, *Phys. Rev. Lett.*, 2008, **100**, 146401.
- 53 A. J. Cohen, P. Mori-Sanchez and W. T. Yang, *Phys. Rev. B: Condens. Matter Mater. Phys.*, 2008, 77, 115123.
- 54 R. W. Godby, M. Schluter and L. J. Sham, *Phys. Rev. B: Condens. Matter Mater. Phys.*, 1987, 35, 4170–4171.
- 55 M.-H. Lee, C.-H. Yang and J.-H. Jan, *Phys. Rev. B: Condens. Matter Mater. Phys.*, 2004, **70**, 235110–235120.
- 56 B. L. Davydov, L. D. Derkacheva, V. V. Dunina, M. E. Zhabotinskii, V. F. Zolin, L. G. Koreneva and M. A. Samokhina, *JETP Lett.*, 1970, 12, 16–18.
- 57 M. J. Frisch, et al., Gaussian 09, Revision D.01, 2009.